NJC

New Journal of Chemistry

An international journal of the chemical sciences

www.rsc.org/njc

Volume 33 | Number 6 | June 2009 | Pages 1157–1440

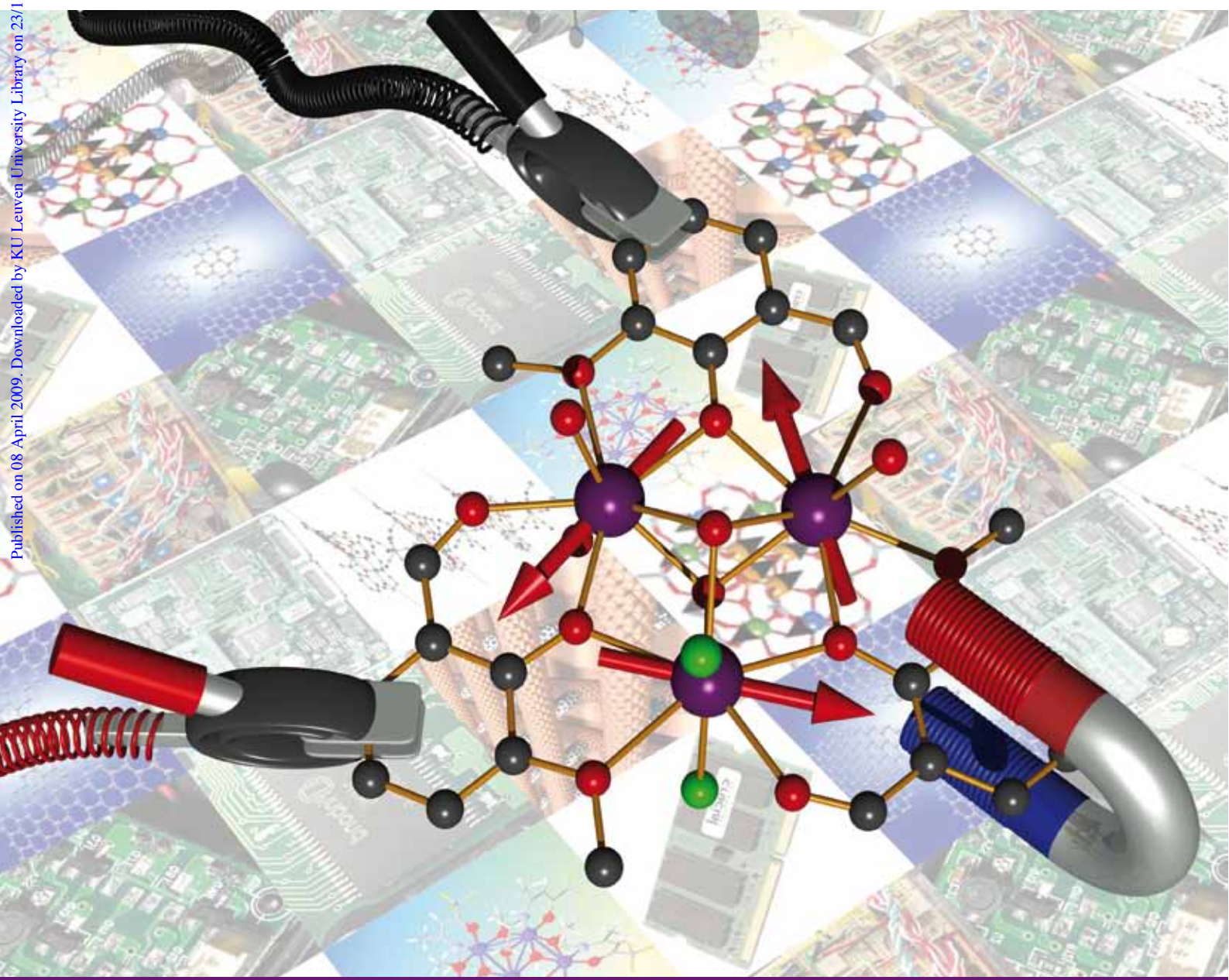

Themed issue: MOLMAT and New Horizons of Photochromism

ISSN 1144-0546

RSC Publishing

PAPER

Liviu F. Chibotaru *et al.*

Ab initio investigation of the non-collinear magnetic structure and the lowest magnetic excitations in dysprosium triangles

Ab initio investigation of the non-collinear magnetic structure and the lowest magnetic excitations in dysprosium triangles

Liviu Ungur,[ab] Willem Van den Heuvel[a] and Liviu F. Chibotaru*[a]

Received (in Montpellier, France) 17th February 2009, Accepted 25th February 2009
First published as an Advance Article on the web 8th April 2009
DOI: 10.1039/b903126j

The unusual magnetism exhibited by dysprosium triangles $[Dy_3(\mu_3\text{-}OH)_2L_3Cl_2(H_2O)_4]$-$[Dy_3(\mu_3\text{-}OH)_2L_3Cl(H_2O)_5]Cl_5\cdot 19H_2O$ is explained using the recently developed *ab initio* methodology for the simulation of magnetic properties of complexes. The local anisotropy axes on the dysprosium sites are found to lie in the plane of the Dy_3 triangle and to make angles of *ca.* 120° with each other. The small antiferromagnetic exchange interaction between sites leads to a non-magnetic Kramers doublet in the ground state of the complex. The arrangement of the local magnetization vectors in this state is close to toroidal. By contrast, the lowest excited states are characterized by a huge magnetic moments of *ca.* 20 μ_B and show very different behavior of magnetization for fields applied along and perpendicular to the plane of the Dy_3 triangle.

Introduction

Anisotropic magnetic molecules with non-collinear spin structure on the metal sites attracted much attention in recent years[1–6] due to new possibilities which they open for tuning the properties of single-molecule magnets[7,8] and single-chain magnets[9,10] and the design of new magnetic materials. Thus spin non-collinearity was shown to be responsible for the existence of transverse anisotropy in axial molecules.[1] The relative orientation of local anisotropy axes was found to influence significantly the coercive field of materials made of single-chain magnets.[11,12] Recent theoretical studies have shown that the non-collinearity of the spin structure influences very strongly the tunneling dynamics in magnetic wheels.[13] Finally, a temperature-induced "anisotropy inversion" phenomenon was found in dysprosium-based single-chain magnets and explained by a peculiar spin canting in these materials.[14]

The determination of anisotropy axes on the metal sites is a relatively simple task if the latter are characterized by some symmetry. For instance, if a metal site has an axial symmetry, the anisotropy axis coincides with the main symmetry axis. Examples are Mn^{3+} ions in octahedral coordination which undergo Jahn–Teller distortions along one of the three tetragonal axes, thus stabilizing the anisotropy axis in the corresponding direction.[15] In the case of relatively simple ligands and weakly distorted complexes the zero-field splitting and the direction of the anisotropy axis can be estimated from ligand-field theory, in particular, using the angular overlap model.[16] However in the case of lanthanides the ligand-field theory is more complex[17] and, therefore, less accurate in its predictions. In addition, the environment of lanthanide ions in a complex usually lack any symmetry, which makes accurate determination of their anisotropic properties almost impossible. Experimentally, the magnetic anisotropy is investigated by inelastic neutron scattering[18,19] and multifrequency high-field EPR,[20,21] however the directions of local anisotropy axes cannot be generally derived by these methods. Also field- and orientation-dependent magnetic susceptibility[14] has been used for the study of anisotropy, *e.g.*, of a Dy-based material, but again, this technique alone does not suffice to resolve the directions of local anisotropy axes.

It seems that the only straightforward way to obtain quantitative information about local (ionic) anisotropy in strongly anisotropic polynuclear complexes and magnetic networks is *via fragment* quantum chemistry calculations taking into account the spin–orbit coupling *non-perturbatively*. In particular, the direction of the local anisotropy axis on a metal site is simply obtained as the main magnetic axis of the *g* tensor of the corresponding Kramers doublet. Some time ago such non-perturbative spin–orbit coupling calculations within the CASSCF/CASPT2 quantum chemistry method have been done for the determination of anisotropy axes on heptacyanomolybdate fragments of cyano bridged Mo(III)Mn(II) networks.[22] The same approach has been successfully applied for the investigation of local anisotropy and the simulation of magnetism in Co(II) dimers[23] and $Co(II)_3Co(III)_4$ heptanuclear wheels.[24]

Recently, three compounds containing a triangle of Dy(III) ions as a central building block, (Fig. 1) $[Dy_3(\mu_3\text{-}OH)_2L_3Cl_2(H_2O)_4][Dy_3(\mu_3\text{-}OH)_2L_3Cl(H_2O)_5]Cl_5\cdot 19H_2O$ (**1**)[25], $[Dy_3(\mu_3\text{-}OH)_2L_3Cl(H_2O)_5]Cl_3\cdot 4H_2O$ (**2**)[25] (where HL = *o*-vanillin) and $[Dy_3Cu_6L_6(\mu_3\text{-}OH)_6(H_2O)_{10}]Cl_2\cdot ClO_4\cdot 3.5H_2O$ (**3**)[26] (where LH_2 = 1,1,1-trifluoro-7-hydroxy-4-methyl-5-azahept-3-en-2-one) have been synthesized and investigated. Compounds **1** and **2** show a vanishing susceptibility at low temperature, which is completely unexpected for systems containing an odd number of electrons. Both these compounds show similar magnetic properties despite the presence of very different magnetic networks,[25] which allows to rule out intermolecular antiferromagnetic exchange interactions as a reason for

[a] *Division of Quantum and Physical Chemistry, Celestijnenlaan 200F, Katholieke Universiteit Leuven, B-3001, Belgium*
[b] *INPAC – Institute for Nanoscale Physics and Chemistry, Celestijnenlaan 200F, Katholieke Universiteit Leuven, B-3001, Belgium. E-mail: Liviu.Chibotaru@chem.kuleuven.be; Fax: +3216-327992; Tel: +3216-327424*

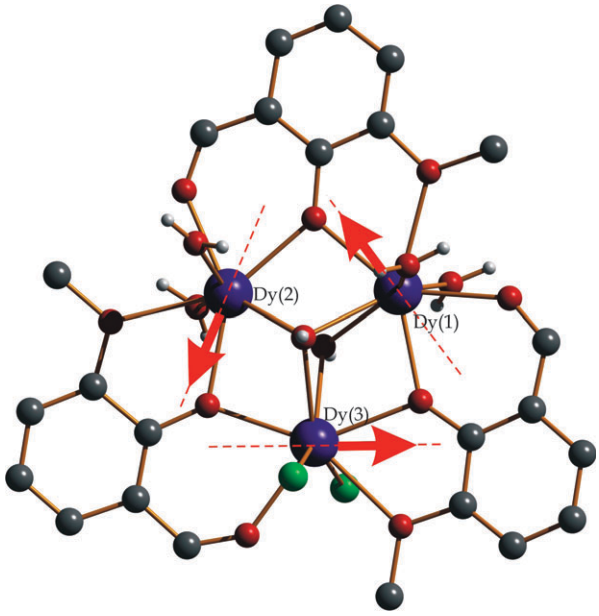

Fig. 1 Structure of the triangular unit in **1** and **2**,[25] containing two chlorides coordinated to Dy(3) sites, which was used in *ab initio* calculations. Color scheme: blue, Dy^{III}; red, O; green, Cl; dark grey, C; white, H. Dashed lines show the calculated anisotropy axes on the dysprosium fragments and the arrows show the ordering of local magnetizations in the ground state of the complex.

vanishing susceptibility at low T. In view of such an unprecedented situation, we have investigated the local anisotropy of dysprosium sites in these complexes by the *ab initio* approach described above and found that the unusual magnetic properties of the dysprosium triangles can be explained by a specific non-collinear magnetic structure of these complexes.[27] Here we give a more detailed description of the local anisotropy on Dy sites and report new *ab initio* investigations of magnetic properties of dysprosium triangles. In particular, we compare our prediction with new experimental data on these complexes.[28]

Computational methodology

In the lanthanide complexes, as in many other metal complexes, the magnetic electrons occupying the 4f orbitals, are well localized at the corresponding metal sites. For these electrons, the crystal-field and the spin–orbit coupling are much stronger than the exchange interactions between different lanthanide centers and therefore should be treated in the first place. On the other hand, the multideterminantal character of the multielectronic wave function of a mononuclear lanthanide fragment (it is essentially the same as for a mononuclear complex) and the subtle competition between crystal-field and spin–orbit coupling in the 4f shell require an explicitly correlated *ab initio* method for their treatment. Following these considerations, for the simulation of magnetic properties of polynuclear complexes we used a computational methodology which combines *ab initio* calculations of mononuclear fragments with a model description of the exchange interaction between different fragments.

The *ab initio* calculations of mononuclear fragments have been done within the CASSCF/CASPT2/RASSI-SO approach implemented in the MOLCAS 7.0 package.[29] The obtained wave functions and energies of the molecular multiplets have been used for the calculations of anisotropic magnetic properties and the g tensors for the lowest Kramers doublets of individual lanthanide fragments using a specially designed routine SINGLE_ANISO.[30] Thus, the magnetic properties of individual metal ions are treated by a parameter-free *ab initio* approach, in which the spin–orbit interaction is taken into account in a non-perturbative way.

The description of anisotropic exchange interaction between metal sites was done within the Lines model.[31] It approximates the isotropic exchange interaction between different spin terms of a given pair of fragments, which arise in the absence of spin–orbit interaction, by a single–parameter exchange Hamiltonian. Diagonalizing the matrix of this Heisenberg Hamiltonian, written in the basis of spin–orbit multiplets of mononuclear metal fragments, obtained from quantum chemistry calculations, gives solutions corresponding to anisotropic exchange interactions between Kramers doublets of a given metal pair. The main advantage of the Lines model is that it uses only one single parameter corresponding to effective isotropic exchange interaction to simulate the anisotropic exchange coupling for each pair of fragments. The important feature of this approximation is that it can be systematically improved by specifying different exchange parameters for relevant spin terms on the fragment. In some cases, as in the present case of Dy_3 complexes, the Lines model is completely adequate as emphasized below. The simulations of the exchange spectrum have been done with a specially designed routine POLY_ANISO,[30] which was interfaced with the SINGLE_ANISO routine treating individual metal fragments. The obtained exchange spectrum and the corresponding wave functions of the polynuclear complex have been used for the calculation of temperature- and field-dependent magnetic properties of the polynuclear complex within the same routine POLY_ANISO.

Results and discussion

Ab initio calculations of Dy(III) fragments

Overview of the structures. The main structural difference between the triangular units in **1** and **2** (Fig. 1) is the Dy(3) site, which is coordinated by one chloride ion above and one water molecule below the plane of the triangle in **1** whilst in **2** this site is occupied by a chloride ion above the plane and a chloride ion or a water molecule below the plane with a 50 : 50 disorder. Since the magnetic data for **1** and **2** practically do not differ,[25] we may conclude that the substitution of the water molecule by a chloride ion on the Dy(3) site will not change the magnetic properties of the Dy_3 unit and consider further the complex with the Dy(3) unit coordinated by two chlorides (Fig. 1).

Computational details. First, we should remove suitable mononuclear fragments from the complex, which would not change significantly the energy structure on the magnetic centers. To have a good description of the 4f ligand–field

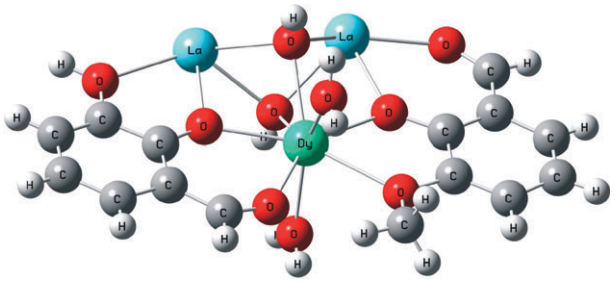

Fig. 2 The structure of the calculated fragments of centers Dy(1) and Dy(2). In the fragment of the center Dy(3), the main difference is that the out of plane chlorine ions substitute the water molecules.

states within a fragment one needs to take into account the influence of the neighboring dysprosium ions. They have been simulated by the closed–shell La^{3+} *ab initio* embedding model potentials (AIMP).[32] Our second concern is the dimension of the coordination sphere. Cutting the distant atoms may have a crucial effect on the orientation of anisotropy axes. Therefore, we took into account all distant atoms with a small basis sets, thus making possible to take larger basis sets for dysprosium and the atoms from the first coordination sphere. The only removed atoms are those from one *o*-vanillin group and the out of plane ligands connected to the two Dy^{3+} ions which we replaced by La^{3+} AIMP. The structure of one of the calculated fragments is shown in Fig. 2. No geometry optimization of the fragments has been done, all atomic coordinates (except for added hydrogen atoms) being taken from the crystal X-ray analysis.

The basis sets were taken from the MOLCAS ANO-RCC library for dysprosium and the atoms from the first coordination sphere, while for the distant atoms smaller relativistic atomic natural orbital basis sets from the ANO-DK3 basis library were used.[33] The following contractions were used: [8s7p5d4f2g1h] for Dy, [3s2p1d] for O, [4s3p1d] for Cl, [2s1p] for H. Embedding potential $La^{3+}/LaMnO_3$ were used to simulate the influence of the neighbor Dy ions.[34]

The active space for the complete active space self-consisting field (CASSCF) calculation included the Dy 4f orbitals (CAS (9 in 7)) since we are interested in the ligand field states only. The charge transfer states have not been calculated because they lie much higher in energy and thus are irrelevant for magnetism. Since the lanthanides have a very strong spin–orbit coupling, a large number of roots should be included in the spin–orbit mixing within the restricted active space state interaction (RASSI-SO) procedure. Accordingly, for each dysprosium fragment we performed CASSCF calculations including the effects of spin–orbit coupling by mixing all terms with energies $<50\,000$ cm^{-1}. These originate from the following Dy^{3+} atomic terms: ^{6}H, ^{6}F, and ^{6}P (all sextets); ^{4}I, ^{4}F, ^{4}M, ^{4}G, ^{4}K, ^{4}L, ^{4}D, ^{4}H, ^{4}P, ^{4}G, ^{4}F and ^{4}I (128 from 224 quadruplets); ^{2}L ,^{2}K, ^{2}P, ^{2}N, ^{2}F, ^{2}M, ^{2}H, ^{2}D, ^{2}G and ^{2}O (130 from 490 doublets). An important aspect of the lanthanide state interaction calculation is that one should take into account all the roots coming from a given multiplet: taking fewer of them may induce strong deviations. The second-order multi-configurational perturbation calculation (CASPT2) was not performed. It was only tested for the lowest 20–30 roots in order to estimate the average change in the energy differences. It turns out that the CASPT2 relative energies do not differ much from the CASSCF ones, therefore, the CASSCF energies were further used.

Local *g* tensors and anisotropy axes. As expected, we obtain for the lowest states of each dysprosium site a group of eight Kramers doublets, originating mainly from the ground multiplet $^6H_{15/2}$ of Dy^{3+} ion, (Table 1) separated by $\sim$3000 cm^{-1} from other excited states. As is shown in Table 1, the ground Kramers doublet is separated by a relatively large gap ($\geq$150 cm^{-1}) from the first excited doublet.

Using the obtained multiplet wave functions, we calculated the *g* tensors of the three dysprosium fragments in the ground Kramers doublet with the described methodology.[30] The main values of the *g* tensors, corresponding to an effective spin $\tilde{s} = 1/2$ of the Kramers doublet, are listed in Table 1. We can see that the obtained *g* tensors are very anisotropic and resemble closely the *g* tensors of the Kramers doublet of a pure $|M_J = \pm 15/2\rangle$ type,[35] despite the lack of axial symmetry on sites (Fig. 1). The calculated directions of the anisotropy axes on three dysprosium sites are shown in Fig. 1 by dashed lines. The three axes form an almost perfect equilateral triangle and lie practically in the Dy_3 plane (the deviation angles are listed in Table 2). Their deviations from tangential directions (Scheme 1) are also quite small (last line in Table 2).

Within the same *ab initio* approach,[30] we calculated the magnetic susceptibility of individual dysprosium fragments (Fig. 3, dashed line).

Magnetic properties of the dysprosium triangles

Simulation of magnetism. The exchange interaction between dysprosium sites has been simulated within the Lines model, in which the effective Heisenberg Hamiltonian, $H_{ex} = -\sum_{i=1}^{3} J_i \boldsymbol{S}_i \cdot \boldsymbol{S}_{i+1}$, corresponding to local spins $S_i = 5/2$ on dysprosium sites, was diagonalized in the basis of Kramers doublets obtained in fragment *ab initio* calculations. This approach is completely adequate in the present case because the local Kramers doublets are found to be close to $|M_J = \pm 15/2\rangle$. In this case, given the smallness of exchange interactions, compared to local excitation energies on sites (Table 1), we expect the exchange interaction to be of Ising type:

$$\tilde{H}_{ex} = -\sum_{i=1}^{3} \tilde{J}_i \tilde{s}_{iz} \tilde{s}_{i+1z} \qquad (1)$$

since the contribution of the terms connecting the states $|+15/2\rangle$ and $|-15/2\rangle$ is negligible for small exchange between sites.[13,20]

Table 1 Lowest calculated Kramers doublets of three dysprosium fragments (cm^{-1})

KD	Dy(1)	Dy(2)	Dy(3)
1	0.0	0.0	0.0
2	234.2	217.8	150.2
3	373.3	367.0	208.1
4	449.0	479.3	258.2
5	501.2	532.0	336.8
6	554.4	638.1	435.6
7	657.9	684.5	579.9
8	741.4	763.0	707.5

Table 2 The calculated g tensors and anisotropy axes for the lowest Kramers doublets of the three dysprosium fragments

Dy(1)	Dy(2)	Dy(3)
0.003	0.003	0.064
0.005	0.004	0.089
19.844	19.837	19.740
Angle of anisotropy axis with Dy_3 plane:		
−4.3°	8.8°	−2.4°
Angle of anisotropy axis with tangential direction ϕ_i:		
8.87°	9.49°	8.72°

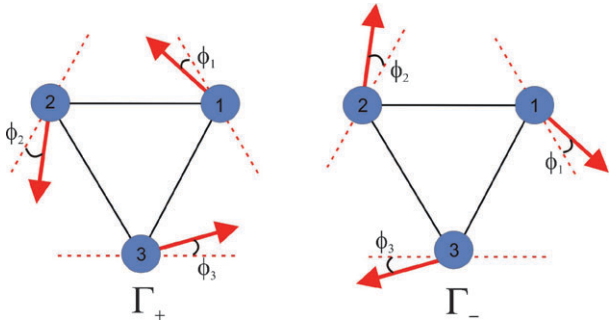

Scheme 1 The two components of the ground Kramers doublet in **1** and **2**. The arrows show the direction of magnetization on dysprosium sites. The angles ϕ_I represent the deviation of the corresponding local anisotropy axis from the tangential direction. Their values are given in Table 2.

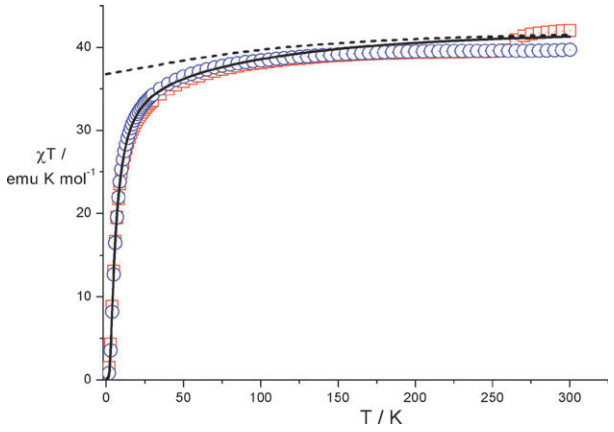

Fig. 3 Temperature dependence of the magnetic susceptibility multiplied by temperature per Dy_3 molecule calculated as a sum of independent dysprosium fragments (--) and simulated for $J = -0.6$ cm^{-1} (—) for a polycrystalline sample and the experimental powder χT values[25] for **1** (□) and **2** (○).

In this equation, $\tilde{s}_{iz}$ is the projection of the pseudo-spin on the anisotropy axis of site i (Fig. 1), describing the two states with (opposite) maximal magnetization on this site. Within the Lines model we come to the same Ising interaction (1) with $\tilde{J}_i = 25\cos\varphi_{i,i+1}J_i$, where $\varphi_{i,i+1}$ is the angle between the anisotropy axes on sites i and $i + 1$. Since $\varphi_{i,i+1} \approx 2\pi/3$ (Fig. 1), we have $\tilde{J}_i \approx -12.5J_i$. Given the magnetic similarity of dysprosium fragments obtained in *ab initio* calculations, we suppose further $J_i = J$ ($\tilde{J}_i = \tilde{J}$).

The simulated powder magnetic susceptibility and magnetization for $J = -0.6$ cm^{-1}, ($\tilde{J} = 7.5$ cm^{-1})—the only fitting parameter of the theory, are shown in Fig. 3 and 4, respectively. The calculated susceptibility and magnetization compare very well with experiment,[25] thus justifying the single-parameter approximation of the exchange interaction.

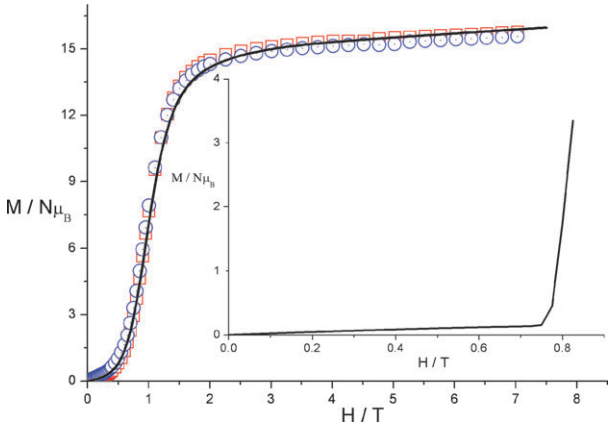

Fig. 4 Molar magnetization *vs.* the applied magnetic field calculated for $J = -0.6$ cm^{-1} (—) for a polycrystalline sample and the experimental powder magnetization[25] for **1** (□) and **2** (○) for $T = 1.8$ K. Inset: the same simulations for $T = 0.1$ K.

Magnetic anisotropy of dysprosium triangles. As a result of highly anisotropic local sites, the whole molecule Dy_3 also shows pronounced magnetic anisotropy. Indeed, the calculated magnetic susceptibility is found to be strongly different for in-plane direction (curves X and Y in Fig. 5), and the perpendicular direction (curve Z in Fig. 5). The same can be said about the single-crystal magnetization; it depends strongly on the direction of the applied magnetic field (Fig. 6). From the calculated low-temperature magnetization (Fig. 7) it is evident that spin flip transitions (level crossings) occur in Dy_3 for certain values of field.

Thus, the in-plane applied field induces a spin flip transition at *ca.* 0.8 T (red curve in Fig. 7), while in the field oriented perpendicular to the plane of the dysprosium triangle such a transition appears at much stronger fields (blue curve in Fig. 7).

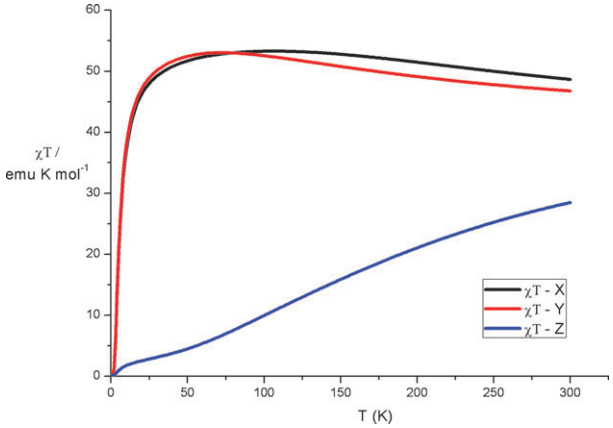

Fig. 5 Temperature dependence of the magnetic susceptibility in the directions of the main magnetic axes of the ground Kramers doublet of the Dy_3 complex. The average over these curves gives the solid line in Fig. 3.

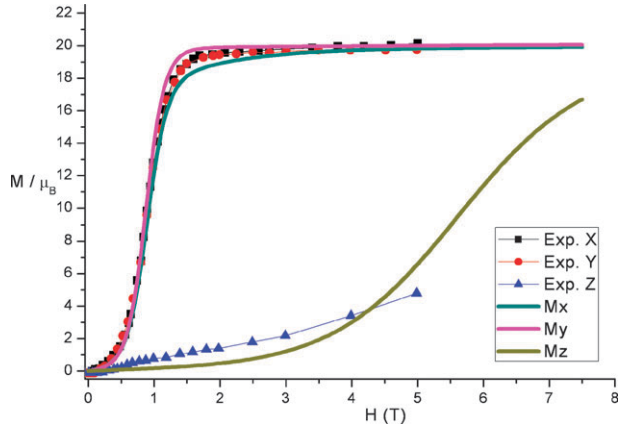

Fig. 6 A comparison between the calculated molar magnetization (bold lines) of the Dy_3 at 1.9 K with the experimental data.[28]

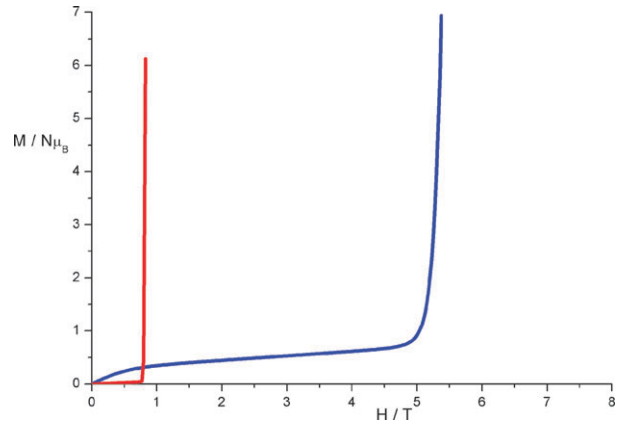

Fig. 7 Single-crystal molar magnetization of the Dy_3 at 0.1 K when the magnetic field is oriented: (a) in the plane of Dy_3 (red line) and (b) perpendicular to the plane of Dy_3 (blue line).

Ground magnetic state: evidence for an almost toroidal magnetic moment on dysprosium triangles. We can see that χT almost vanishes at low temperature, which means an almost non-magnetic ground state. The origin of this state is easy to understand: for antiferromagnetic J we have $\tilde{J} > 0$ and eqn (1) predicts a ferromagnetic alignment of the pseudo-spins (and local magnetization vectors) along the anisotropy axes, as shown in Fig. 1 by arrows. Since the local magnetization vectors are almost tangential to the vertices of the Dy_3 triangle we have here an example of an almost perfect toroidal magnetic moment. The second component of the Kramers doublet is obtained by time inversion operation, which changes the directions of all magnetic moments (Scheme 1).

Origin of the in-plane alignment of anisotropy axes. The arrangement of the eight atoms that coordinate each Dy ion approximates that of a trigonal dodecahedron. This structure has D_{2d} symmetry and originates from the cube by respectively elongating and compressing the cube's two tetrahedra along a fourfold axis, which becomes the D_{2d} main axis. In the Dy_3 molecule, this axis, which we will call here the z-axis, is directed radially outward at each Dy site. In this idealized symmetry, the x- and y-directions are equivalent. Therefore, the main anisotropy axis of a highly anisotropic ground state on a Dy site would necessarily have to coincide with the z-axis, that is, pointing outward the triangle. Indeed, a crystal-field calculation for the $J = 15/2$ multiplet, based on a point-charge potential with equal charges on the eight coordinating atoms, yields an almost pure $M_J = \pm 15/2$ ground doublet with anisotropy axis in the z-direction. A configuration of this kind leads to a non-magnetic ground state of the Dy_3 molecule but does not agree with the almost tangential configuration of the *ab initio* results (Fig. 1 and Scheme 1). To obtain the latter in a crystal-field model, a higher effective negative charge has to be attributed to the two oxygen atoms lying closest to the tangential axis (these are the hydroxy-oxygens of the *o*-vanillin ligands, see Fig. 1), thereby breaking the D_{2d} symmetry. A 50% increase of these charges indeed leads to the desired ground doublet with tangential anisotropy axis and g-factor between 19 and 20. In a crystal-field model, effective point charges account both for electrostatic and for covalent interaction. The present finding suggests that the two considered oxygen atoms exert a stronger ligand-field effect than the other six. This is possibly due to the combination of the negative charge of the oxy-group and the σ-bonding effect of the directed sp_2-lone pair.

Comparison with the model treatment by Luzon *et al.*[28] Recently single-crystal magnetic studies have been reported for **1**.[28] These additional data allowed the fitting of magnetism by a simple model. The model[28] involved the exchange interaction equivalent to eqn (1), a rotationally symmetric arrangement of in-plane local anisotropy axes ($\phi_i = \phi$) and the exchange interaction described by one g factor for all three dysprosium sites. The model contained four fitting parameters, $\tilde{J}$, g, ϕ and δ—the energy gap to the first excited Kramers doublet on dysprosium sites. The lowest and first excited Kramers doublets on dysprosium sites were assumed to be of pure $|15/2, \pm 15/2\rangle$ and $|15/2, \pm 13/2\rangle$ type, respectively, with quantization axes along corresponding local anisotropy axes. One of the fitted values of ϕ (the fitting gave several equivalent values of ϕ due to high symmetry of the model[28]) corresponds to $\phi = 13°$, which compares very well with the *ab initio* values $\phi_i = 8.7$–$9.5°$ in Table 2. The same applies for the fitted values of g, when it is recalculated for $\tilde{s} = 1/2$, and the parameter $\tilde{J}$. However the fitting of δ gave a value of 71 cm^{-1} which is substantially lower than the energy separations between the ground and the first excited Kramers doublets on dysprosium sites listed in Table 1. We note that the two lowest Kramers doublets are actually not characterized by a definite projection of the total angular moment on the anisotropy axis (this would be only possible in the presence of a high order rotational axis on sites). However, the main reason for this discrepancy is that only two Kramers doublets on the dysprosium sites have been used for the simulation of magnetism in ref. 28, which is not enough for Dy^{3+} complexes. To illustrate this point we compare in Fig. 8 our previous simulations of susceptibility and magnetization of Dy_3, when all Kramers doublets on dysprosium sites up to 50 000 cm^{-1} were taken into account (upper curves), with the

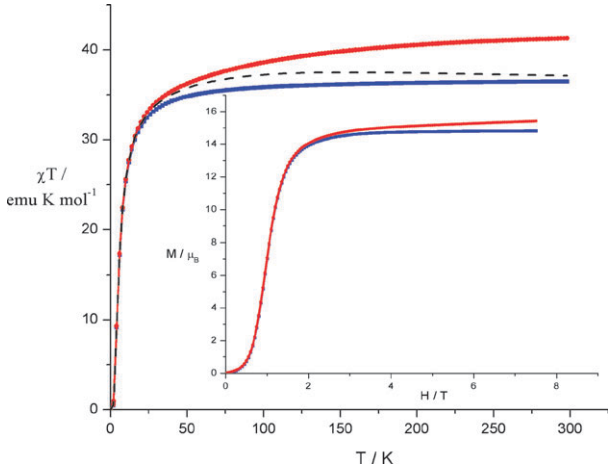

Fig. 8 A comparison of the magnetic susceptibility (χT) arising from the interaction of all states on Dy sites (upper red line), two Kramers doublets from each site (dashed line) and only the ground Kramers doublets from each site (lower blue line). The difference between these curves represents the contribution to the magnetic susceptibility coming from excited states. Inset: the same simulations for the molar magnetization at $T = 1.8$ K.

simulations taking into account only the ground Kramers doublets on sites (lower curves) and the lower and first excited Kramers doublets (dashed line).

Despite this discrepancy, our *ab initio* treatment and the model simulations in ref. 28 give essentially the same description of the magnetism of dysprosium triangles. This agreement is reassuring since it gives strong evidence for the correctness of the interpretation of magnetic properties of these compounds and the capability of our *ab initio* based methodology to describe the magnetism of strongly anisotropic complexes.

Lowest magnetic excitations in dysprosium triangles. Fig. 4 (inset) shows that even at very low temperature the magnetization is not zero but increases with field and comes almost to saturation before rising steeply at $H \approx 0.8$ T. This points out to a remnant small magnetic moment in the ground state. Fig. 9 shows the evolution of four exchange Kramers doublets of Dy_3, arising from the exchange interaction between lowest Kramers doublets on dysprosium sites, in a magnetic field. The ground Kramers doublet splits almost linearly with field applied perpendicular to the plane and shows no splitting for the in-plane direction of the field, which means that the non-compensated magnetic moment is directed perpendicular to the plane. Accordingly, the calculated g tensor for the ground Kramers doublet (Table 3) has the main magnetic axis directed perpendicular to the Dy_3 plane. The lowest excited Kramers doublets correspond to reversal of the direction of magnetization on one of the three dysprosium sites, respectively (states 2–4 in Fig. 9(c)). According to eqn (1) their excitation energies $\approx \tilde{J} = 7.5$ cm^{-1}, which is indeed seen in Fig. 9 (energy levels at zero field). In addition, in each of these states the complex acquires a magnetic moment of *ca.* twice the moment of an individual dysprosium site *i.e.* $\approx 19.7\ \mu_B$. As a result, close to the crossing fields a step rise of magnetization occurs (Fig. 7). As Fig. 9 shows, these

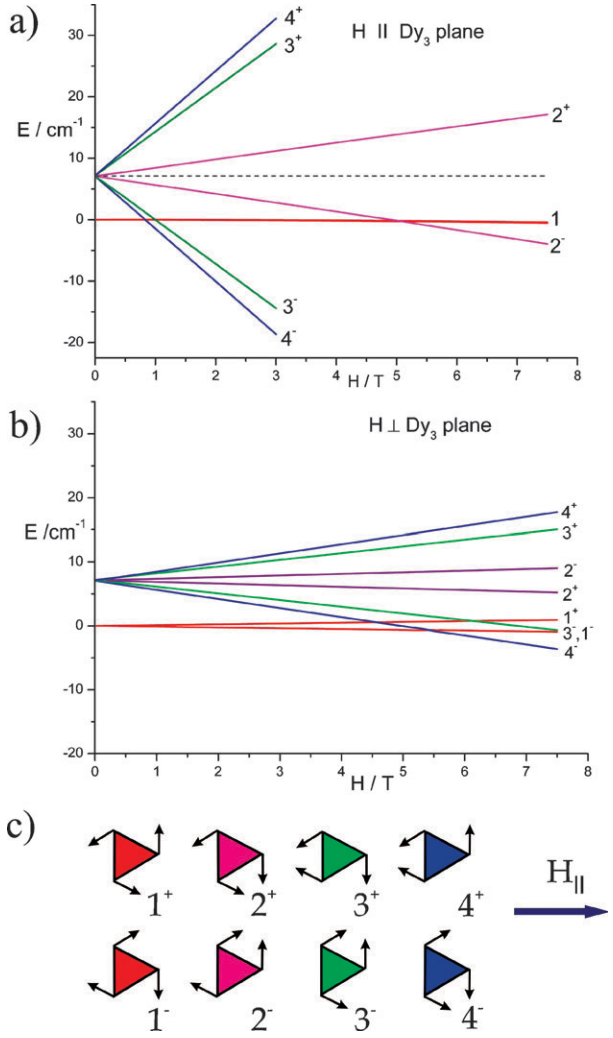

Fig. 9 Evolution of the lowest magnetic states of Dy_3 complex with applied magnetic field, simulated for $J = -0.6$ cm^{-1}: (a) H is perpendicular to the Dy_3 plane; (b) H is applied in the Dy_3 plane. (c) Schematic non-collinear magnetic structure of the ground (4) and three excited (1–3) Kramers doublets and the direction of the in-plane applied field in (a). The two signs in the superscripts denote the two time-reversal components of the Kramers doublets.

Table 3 The calculated g tensors for the lowest and three excites Kramers doublets of the dysprosium triangle

KD	g_1	g_2	g_3
1	0.000000	0.000000	0.558
2	0.000084	0.006237	39.290
3	0.000147	0.001894	37.732
4	0.000065	0.004267	37.963

crossing fields differ several times for in plane and perpendicular to the plane directions, which means that the Dy_3 plane is the easy plane of magnetization. The splitting of the pairs $(3^+,4^+)$, $(3^-,4^-)$ and $(2^+,2^-)$ in Fig. 9(a) is caused by the deviations of the local anisotropy axes from the tangential direction.

In an idealized situation where the local anisotropy axes lie perfectly in the Dy_3 plane there should be no linear splitting of

the ground and excited Kramers doublets when the magnetic field is oriented perpendicular to the plane. The calculations have shown the presence of the uncompensated moment in the perpendicular direction, which interacts with the magnetic field to produce the Zeeman splitting in the energy levels in both ground and excited Kramers doublets. These are clearly seen in Fig. 9(b).

Conclusions

We have presented here the application of a recently developed *ab initio* based methodology for the description of magnetic properties of dysprosium(III) triangles. The unusual magnetic properties of dysprosium triangles are explained by a peculiar (almost toroidal) alignment of the local anisotropy axes on the three dysprosium sites (Scheme 1). We have found good agreement between the calculated directions of local anisotropy axes with those derived from experiment, which gives credibility to our *ab initio* method. The ground Kramers doublets on dysprosium sites support an Ising exchange interaction, preserving the state of maximal magnetization on the sites. Reversing the toroidal magnetization requires consecutive transitions through two of the three excited Kramers doublets of Dy_3 *e.g.* $1^+ \rightarrow 2^+ \rightarrow 3^+ \rightarrow 1^-$. The very low values of the calculated two perpendicular g components on the dysprosium sites point to the possibility of blocking of this toroidal magnetization, which is supported by recently reported slow relaxation of magnetization in these complexes.[28]

Acknowledgements

L. U. thanks the financial support of the Flemish Government under concerted action scheme and the grant EF/05/005 (INPAC) from the Katholieke Universiteit of Leuven. Willem Van den Heuvel is "Aspirant van het FWO". A. Soncini, R. Sessoli and A. K. Powell are gratefully acknowledged for useful discussions.

References

1 A. L. Barra, A. Caneschi, A. Cornia, D. Gatteschi, L. Gorini, L. P. Heiniger, R. Sessoli and L. Sorace, *J. Am. Chem. Soc.*, 2007, **129**, 10754–10762.
2 K. Bernot, J. Luzon, R. Sessoli, A. Vindigni, J. Thion, S. Richeter, D. Leclercq, J. Larionova and A. van der Lee, *J. Am. Chem. Soc.*, 2008, **130**, 1619–1627.
3 T. Kajiwara, M. Nakano, Y. Kaneko, S. Takaishi, T. Ito, M. Yamashita, A. Igashira-Kamiyama, H. Nojiri, Y. Ono and N. Kojima, *J. Am. Chem. Soc.*, 2005, **127**, 10150–10151.
4 A. M. Madalan, K. Bernot, F. Pointillart, M. Andruh and A. Caneschi, *Eur. J. Inorg. Chem.*, 2007, 5533–5540.
5 G. Poneti, K. Bernot, L. Bogani, A. Caneschi, R. Sessoli, W. Wernsdorfer and D. Gatteschi, *Chem. Commun.*, 2007, 1807–1809.
6 X. Y. Wang, Z. M. Wang and S. Gao, *Inorg. Chem.*, 2008, **47**, 5720–5726.
7 D. Gatteschi and R. Sessoli, *Angew. Chem., Int. Ed.*, 2003, **42**, 268–297.
8 D. Gatteschi, R. Sessoli and J. Villain, *Molecular Nanomagnetism*, Oxford University Press, Oxford, 2006.
9 A. Cornia, A. F. Costantino, L. Zobbi, A. Caneschi, D. Gatteschi, M. Mannini and R. Sessoli, *Struct. Bonding*, 2006, **122**, 133–161.
10 C. Coulon, H. Miyasaka and R. Clerac, *Struct. Bonding*, 2006, **122**, 163–206.
11 N. Ishii, Y. Okamura, S. Chiba, T. Nogami and T. Ishida, *J. Am. Chem. Soc.*, 2008, **130**, 24–25.
12 R. Sessoli, *Angew. Chem., Int. Ed.*, 2008, **47**, 5508–5510.
13 A. Soncini and L. F. Chibotaru, *Phys. Rev. B*, 2008, **77**, 220406.
14 K. Bernot, J. Luzon, A. Caneschi, D. Gatteschi, R. Sessoli, L. Bogani, A. Vindigni, A. Rettori and M. G. Pini, 2009, arXiv:0901.4409 [cond-mat.mtrl-sci].
15 J. S. Griffith, *The Theory of Transition Metal Ions*, Cambridge University Press, Cambridge, 1971.
16 D. Gatteschi and L. Sorace, *J. Solid State Chem.*, 2001, **159**, 253–261.
17 A. K. Zvezdin, V. M. Matveev, A. A. Mukhin and A. I. Popov, *Rare-Earth Ions in Ordered Magnetic Crystals*, Nauka, Moscow, 1985.
18 H. U. Gudel, U. Hauser and A. Furrer, *Inorg. Chem.*, 1979, **18**, 2730–2737.
19 G. Amoretti, R. Caciuffo, S. Carretta, T. Guidi, N. Magnani and P. Santini, *Inorg. Chim. Acta*, 2008, **361**, 3771–3776.
20 A. Bencini and D. Gatteschi, *EPR of Exchange Coupled Systems*, Springer-Verlag, New York, 1990.
21 A. L. Barra, D. Gatteschi, R. Sessoli, G. L. Abbati, A. Cornia, A. C. Fabretti and M. G. Uytterhoeven, *Angew. Chem., Int. Ed.*, 1997, **36**, 2329–2331.
22 L. F. Chibotaru, M. F. A. Hendrickx, S. Clima, J. Larionova and A. Ceulemans, *J. Phys. Chem. A*, 2005, **109**, 7251–7257.
23 S. Petit, G. Pilet, D. Luneau, L. F. Chibotaru and L. Ungur, *Dalton Trans.*, 2007, 4582–4588.
24 L. F. Chibotaru, L. Ungur, C. Aronica, H. Elmoll, G. Pilet and D. Luneau, *J. Am. Chem. Soc.*, 2008, **130**, 12445–12455.
25 J. K. Tang, I. Hewitt, N. T. Madhu, G. Chastanet, W. Wernsdorfer, C. E. Anson, C. Benelli, R. Sessoli and A. K. Powell, *Angew. Chem., Int. Ed.*, 2006, **45**, 1729–1733.
26 C. Aronica, G. Pilet, G. Chastanet, W. Wernsdorfer, J. F. Jacquot and D. Luneau, *Angew. Chem., Int. Ed.*, 2006, **45**, 4659–4662.
27 L. F. Chibotaru, L. Ungur and A. Soncini, *Angew. Chem., Int. Ed.*, 2008, **47**, 4126–4129.
28 J. Luzon, K. Bernot, I. J. Hewitt, C. E. Anson, A. K. Powell and R. Sessoli, *Phys. Rev. Lett.*, 2008, **100**, 247205.
29 G. Karlstrom, R. Lindh, P. A. Malmqvist, B. O. Roos, U. Ryde, V. Veryazov, P. O. Widmark, M. Cossi, B. Schimmelpfennig, P. Neogrady and L. Seijo, *Comput. Mater. Sci.*, 2003, **28**, 222–239.
30 L. F. Chibotaru and L. Ungur, *The computer programs SINGLE_ANISO and POLY_ANISO*, University of Leuven, 2006.
31 M. E. Lines, *J. Chem. Phys.*, 1971, **55**, 2977.
32 L. Seijo and Z. Barandiaran, in *Computational Chemistry: Reviews of Current Trends*, ed. L. J., World Scientific, Singapore, 1999, pp. 55–152.
33 T. Tsuchiya, M. Abe, T. Nakajima and K. Hirao, *J. Chem. Phys.*, 2001, **115**, 4463–4472.
34 A. Sadoc, R. Broer and C. de Graaf, *J. Chem. Phys.*, 2007, **126**.
35 J. Hog and P. Touborg, *Phys. Rev. B*, 1975, **11**, 520–529.

